

involve

a journal of mathematics

Analysis of steady states for classes of reaction-diffusion
equations with hump-shaped density-dependent dispersal on
the boundary

Quinn Morris, Jessica Nash and Catherine Payne



Analysis of steady states for classes of reaction-diffusion equations with hump-shaped density-dependent dispersal on the boundary

Quinn Morris, Jessica Nash and Catherine Payne

(Communicated by Kenneth S. Berenhaut)

We study a two-point boundary-value problem describing steady states of a population dynamics model with diffusion, logistic growth, and nonlinear density-dependent dispersal on the boundary. In particular, we focus on a model in which the population exhibits hump-shaped density-dependent dispersal on the boundary, and explore its effects on existence, uniqueness and multiplicity of steady states.

1. Introduction

Since the early work of Fisher [1937] and Kolmogorov, Petrovskii, and Piskunov [Kolmogorov et al. 1937], differential equations models have been used to model the dynamics of a population inhabiting a patch. Since their early work, the models have grown in complexity with the goal of understanding long-term persistence of populations through the analysis of such models. In a one-dimensional patch $\Omega = (0, \ell)$ for some $\ell > 0$ such models take the form

$$\begin{aligned} u_t &= Du_{\tilde{x}\tilde{x}} + u\tilde{f}(u), & \tilde{x} \in \Omega, t > 0, \\ B_1u(0, t) &= 0, & t > 0, \\ B_2u(\ell, t) &= 0, & t > 0, \\ u(\tilde{x}, 0) &= u_0(\tilde{x}), \end{aligned} \tag{1}$$

where $u(\tilde{x}, t)$ is the population density at point $\tilde{x} \in \Omega$ at time $t > 0$, D is a diffusion rate within the habitat, $\tilde{f} : (0, \infty) \rightarrow (-\infty, \infty)$ is the per-capita growth rate, B_1 and B_2 are boundary operators (possibly nonlinear), and $u_0 : [0, \ell] \rightarrow [0, \infty)$ is an initial population distribution. Such models are often referred to as “reaction-diffusion models” as the rate of change of the population density (u_t) is determined by both a

MSC2010: 34B18, 34C60, 92D25.

Keywords: differential equation, mathematical ecology, nonlinear dispersal, nonlinear boundary condition, logistic equation, reaction-diffusion equation, density-dependent dispersal.

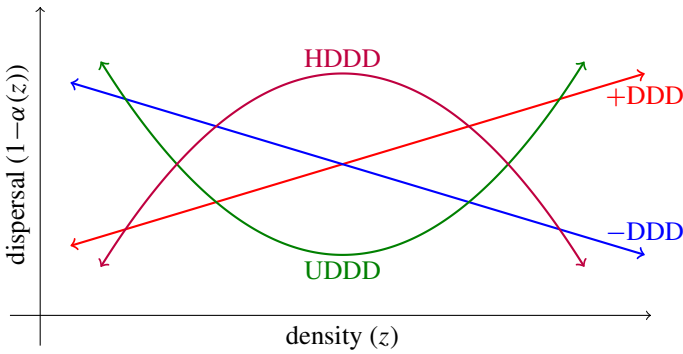


Figure 1. Graphs of possible density-dispersal relations, where z is population density and $1 - \alpha(z)$ is the probability of dispersal from the patch upon reaching a point on the boundary of where the local population density is z .

reaction term ($u\tilde{f}(u)$), which in this case models the growth of the population, and a diffusion term ($Du_{\tilde{x}\tilde{x}}$), which models movement of the population. The diffusion term $Du_{\tilde{x}\tilde{x}}$ for population movement can be derived from a individual random walk model [Skellam 1951] and is a good fit for modeling movement of many different species [Kareiva 1983; Turchin and Thoeny 1993]. See [Cantrell and Cosner 2003] for the derivation and analysis of a number of models of this form.

In this paper, we consider a reaction-diffusion model of a population in a primary patch Ω which is surrounded by a secondary region (called the matrix, in ecology) with hostility $S^* > 0$ ($S^* \approx 0$ indicates that the matrix is relatively not hostile, while $S^* \gg 0$ indicates that the matrix is relatively more hostile). Such scenarios are common in habitats experiencing fragmentation, whereby large regions of primary habitat are broken into smaller fragments either by destruction of parts of the primary habitat or replacement of the primary habitat by a less suitable matrix. Individuals within the primary patch move via diffusion, and if they reach the boundary, choose to remain in the patch with probability $\alpha(z)$, where $\alpha : [0, \infty) \rightarrow (0, \infty)$ is a function which depends on the population density at the boundary. We note that $1 - \alpha(z)$ gives the dispersal rate of the population from the primary patch, a parameter of interest to ecologists.

There are three main types of density-dependent dispersal $1 - \alpha(z)$ that have been studied; see Figure 1. Specifically, species that demonstrate positive density-dependent dispersal (+DDD) have a low dispersal rate for low densities and a high dispersal rate for high densities. Species of this kind are most likely experiencing crowding effects or lack of resources. Comparatively, for species demonstrating negative density-dependent dispersal (-DDD), there is a higher chance for dispersal when there is a smaller population density. This may be because the species is



Figure 2. Examples of species which have been observed to exhibit $-DDD$ at low densities and $+DDD$ at high densities. Left: blue-footed booby, *Sula nebouxii* (see [Kim et al. 2009]). Image by Bernard Gagnon/CC BY-SA 3.0. Right: Glanville fritillary butterfly, *Melitaea cinxia* (see [Kuussaari et al. 1998] for $-DDD$, and see [Enfjäll and Leimar 2005] for $+DDD$). Photo by Christian Fischer/CC BY-SA 3.0.

experiencing mate scarcity or conspecific attraction. There is also some evidence of species that exhibit $-DDD$ at low densities and $+DDD$ at high densities, which we refer to as u-shaped density-dependent dispersal (UDDD). UDDD has been of recent interest in the mathematical literature, see [Cantrell and Cosner 2003; Cantrell et al. 1998; Cronin et al. 2019; FONSEKA et al. 2019; Goddard et al. 2018; ≥ 2020], as ecologists find evidence that the blue-footed booby and Glanville fritillary butterfly (see Figure 2) exhibit UDDD in nature. In this paper, we are interested in studying species that demonstrate hump-shaped density-dependent dispersal (HDDD), in which species exhibit $+DDD$ at low densities and $-DDD$ at high densities.

We further assume that individuals in the population exhibit logistic growth. In particular, we assume the per-capita growth rate takes the form

$$\tilde{f}(u) = r \left(1 - \frac{u}{K} \right),$$

where $r > 0$ is the maximum population growth rate and $K > 0$ is the carrying capacity such that $\tilde{f}(u) > 0$ for $u \in (0, K)$ and $\tilde{f}(u) < 0$ for $u \in (K, \infty)$.

Based on these assumptions, the resulting model is [Cronin et al. 2019]

$$\begin{aligned} u_t &= Du_{\tilde{x}\tilde{x}} + ru \left(1 - \frac{u}{K} \right), \quad \tilde{x} \in \Omega, \quad t > 0, \\ -D\alpha(u(0, t))u_{\tilde{x}}(0, t) + S^*[1 - \alpha(u(0, t))]u(0, t) &= 0, \\ D\alpha(u(\ell, t))u_{\tilde{x}}(\ell, t) + S^*[1 - \alpha(u(\ell, t))]u(\ell, t) &= 0, \end{aligned} \tag{2}$$

where $u(\tilde{x}, t)$ is the population density at point $\tilde{x} \in \Omega$ at time $t > 0$ and K is the carrying capacity of the population. Rescaling the spatial variable by taking $x = \tilde{x}/\ell$,

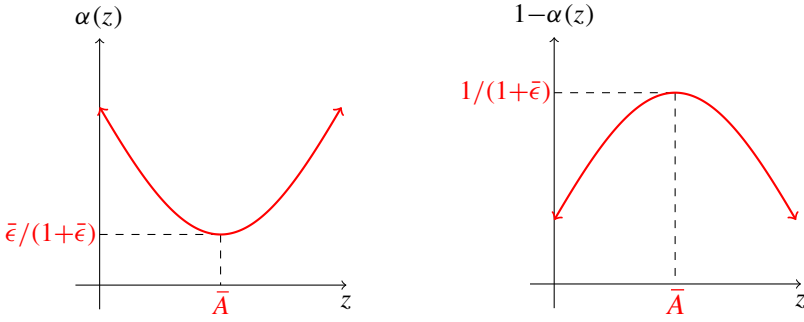


Figure 3. Illustration of relationship between $\alpha(z)$ (left) and dispersal $[1 - \alpha(z)]$ (right). Note that \bar{A} is the density at which the probability of remaining in the patch upon reaching the boundary is at a minimum (in particular, $\alpha(\bar{A}) = \bar{\epsilon}/(1 + \bar{\epsilon})$). Therefore, dispersal on the boundary reaches a maximum of $1 - \alpha(\bar{A}) = 1/(1 + \bar{\epsilon})$ when density is \bar{A} .

we have $u(\tilde{x}, t) = u(x\ell, t) = z(x, t)$, and the model becomes

$$\begin{aligned} z_t &= \frac{D}{\ell^2} z_{xx} + rz \left(1 - \frac{z}{K}\right), \quad x \in (0, 1), \quad t > 0, \\ -\frac{D}{\ell} \alpha(z(0, t)) z_x(0, t) + S^*[1 - \alpha(z(0, t))]z(0, t) &= 0, \\ \frac{D}{\ell} \alpha(z(1, t)) z_x(1, t) + S^*[1 - \alpha(z(1, t))]z(1, t) &= 0, \end{aligned} \quad (3)$$

where $z(x, t)$ is the population density at point $x \in (0, 1)$ at time $t > 0$.

Of particular importance in understanding the dynamics of (3) are the steady states ($\lim_{t \rightarrow \infty} z(x, t)$) of (3). We take $\alpha(z)$ of the form

$$\alpha(z) = \frac{(z - \bar{A})^2 + \bar{\epsilon}}{(z - \bar{A})^2 + (1 + \bar{\epsilon})}$$

for $0 < \bar{A} < K$ and $\bar{\epsilon} > 0$ and examine if steady states of (3) exist. In Figure 3, we note that dispersal $1 - \alpha(z)$ is hump-shaped, as desired, and that the parameter \bar{A} determines the range of population densities on which dispersal is positive density-dependent and negative density-dependent. In particular, if $\bar{A} \approx 0$, then the population exhibits positive density-dependent dispersal for most densities, while if $\bar{A} \approx K$, the population exhibits negative density-dependent dispersal for most densities.

Letting

$$v = \frac{z}{K}, \quad \lambda = \frac{r\ell^2}{D}, \quad \gamma = \frac{S^*}{K^2\sqrt{rD}}, \quad A = \frac{\bar{A}}{K}, \quad \epsilon = \frac{\bar{\epsilon}}{K},$$

we perform a nondimensionalization which yields the one-dimensional problem

$$\begin{aligned} -v'' &= \lambda v(1-v), \quad x \in (0, 1), \\ v'(0) &= \sqrt{\lambda}\gamma \frac{v(0)}{(v(0)-A)^2 + \epsilon}, \\ v'(1) &= -\sqrt{\lambda}\gamma \frac{v(1)}{(v(1)-A)^2 + \epsilon}. \end{aligned} \quad (4)$$

In this paper, we will examine only solutions which are symmetric about $x = \frac{1}{2}$. Note that the following lemma establishes that positive solutions are, in fact, symmetric about $x = \frac{1}{2}$ when $\epsilon > 1 - A^2$.

Lemma 1. *If $\epsilon > 1 - A^2$, then any positive solution v to (4) is symmetric about $x = \frac{1}{2}$; that is, $v(\frac{1}{2} - x) = v(\frac{1}{2} + x)$ for $x \in [0, \frac{1}{2}]$.*

Proof. First, we observe from (4) that any positive solution v of (4) is concave and has exactly one maximum value $x_0 \in (0, 1)$. Furthermore, the solution v of (4) is symmetric about x_0 .

Suppose $x_0 < \frac{1}{2}$, or equivalently $2x_0 < 1$. By symmetry of the solution, let $q_1 = v(2x_0) = v(0) \leq 1$. Then $|v'(2x_0)| = \sqrt{\lambda}\gamma q_1 / ((q_1 - A)^2 + \epsilon)$. Now, let $v(1) = q_2 < q_1$. Then $|v'(1)| = \sqrt{\lambda}\gamma q_2 / ((q_2 - A)^2 + \epsilon)$.

By the assumption that $\epsilon > 1 - A^2$ and $q \leq 1$, we have

$$\frac{d}{dq} \left[\frac{q}{(q-A)^2 + \epsilon} \right] = \frac{A^2 + \epsilon - q^2}{((q-A)^2 + \epsilon)^2} \geq \frac{A^2 + \epsilon - 1}{((q-A)^2 + \epsilon)^2} > 0.$$

Therefore, since $q_2 < q_1$, we must have

$$\frac{q_2}{(q_2 - A)^2 + \epsilon} < \frac{q_1}{(q_1 - A)^2 + \epsilon},$$

which implies $|v'(1)| < |v'(2x_0)|$. But this is a contradiction, since v is concave, and therefore $q_1 = q_2$ and $x_0 = \frac{1}{2}$. \square

For simplicity of notation, we will take $f(s) = s(1-s)$ (the nonlinearity appearing in the differential equation in (4)), and let $F(s) = \int_0^s f(t) dt$. We establish the following theorem:

Theorem 2. *There exists a positive, symmetric solution v to (4) with $\|v\|_\infty = \rho$, $v(1) = q$, and $0 < q < \rho$ if and only if*

$$2 \left(\int_q^\rho \frac{dz}{\sqrt{F(\rho) - F(z)}} \right)^2 = \lambda \quad (5)$$

and

$$\frac{\gamma q}{(q-A)^2 + \epsilon} = \sqrt{2} \sqrt{F(\rho) - F(q)} \quad (6)$$

hold.

In [Section 2](#), we prove [Theorem 2](#) via a quadrature method first introduced in [\[Laetsch 1971\]](#), and recently extended to nonlinear boundary conditions in [\[Goddard et al. 2018; ≥ 2020\]](#). In [Section 3](#), we provide computationally generated bifurcation curves of [\(4\)](#), and in [Section 4](#), we discuss the biological implications of our numerical results.

Remark 3. We emphasize here that [Theorem 2](#) refers only to positive, symmetric solutions of [\(4\)](#). In the case that $\epsilon > 1 - A^2$, by [Lemma 1](#) all positive solutions are symmetric. If, however, $\epsilon \leq 1 - A^2$, then there may be additional nonsymmetric solutions which are not captured by [Theorem 2](#).

2. Proof of [Theorem 2](#)

To prove [Theorem 2](#), we proceed via a quadrature method [\[Laetsch 1971\]](#). We first show that if v is a positive solution to [\(4\)](#) with $\|v\|_\infty = \rho$ and $v(0) = q = v(1)$, then λ , ρ , and q must satisfy [\(5\)](#) and [\(6\)](#). Multiplying both sides of [\(4\)](#) by $v'(x)$ yields

$$\left(\frac{-[v'(x)]^2}{2} \right)' = \lambda(F(v(x)))'. \quad (7)$$

Since $v(\frac{1}{2}) = \rho$ is a maximum and therefore $v'(\frac{1}{2}) = 0$, integrating [\(7\)](#) from s to $\frac{1}{2}$ and rearranging terms gives

$$v'(s) = \sqrt{2\lambda} \sqrt{F(\rho) - F(v(s))}. \quad (8)$$

Integrating [\(8\)](#) from 0 to x and recalling that $v(0) = q$, we obtain

$$\int_q^{v(x)} \frac{dz}{\sqrt{F(\rho) - F(z)}} = \sqrt{2\lambda}x. \quad (9)$$

When $x = \frac{1}{2}$, we have

$$\int_q^\rho \frac{dz}{\sqrt{F(\rho) - F(z)}} = \sqrt{\frac{\lambda}{2}},$$

and hence [\(5\)](#) is satisfied.

Substituting $x = 0$ into [\(8\)](#) and applying the boundary condition in [\(4\)](#) yields

$$\frac{\gamma q}{(q - A)^2 + \epsilon} = \sqrt{2} \sqrt{F(\rho) - F(q)}. \quad (10)$$

Hence, [\(6\)](#) is also satisfied.

We now prove the reverse implication. Let λ , ρ , and q satisfy [\(5\)](#) and [\(6\)](#). We define $v : [0, 1] \rightarrow [0, \rho]$ by [\(9\)](#) if $x \in (0, \frac{1}{2})$, $v(0) = q$, and $v(x) = v(x - \frac{1}{2})$ if $x \in (\frac{1}{2}, 1]$.

Note that $\sqrt{2\lambda}x$ increases from 0 to

$$\int_q^\rho \frac{dz}{\sqrt{F(\rho) - F(z)}}$$

as x increases from 0 to $\frac{1}{2}$. Similarly,

$$\int_q^v \frac{dz}{\sqrt{F(\rho) - F(z)}}$$

increases from 0 to

$$\int_q^\rho \frac{dz}{\sqrt{F(\rho) - F(z)}}$$

as v increases from q to ρ . Hence, $v(x)$ is well defined for $x \in (0, \frac{1}{2})$.

Defining $H : (0, \frac{1}{2}) \times (q, \rho) \rightarrow \mathbb{R}$ by

$$H(\tau, v) = \int_q^v \frac{dz}{\sqrt{F(\rho) - F(s)}} - \sqrt{2\lambda}\tau,$$

we observe that $H \in C^1((0, \frac{1}{2}) \times (q, \rho))$, $H(x, v(x)) = 0$ for $x \in (0, \frac{1}{2})$, and

$$\left. \frac{\partial H}{\partial v} \right|_{(t, v(t))} = \frac{1}{\sqrt{F(\rho) - F(v(t))}} > 0.$$

By the implicit function theorem, we may therefore conclude that $v \in C^1(0, \frac{1}{2})$. From (9), we may now write

$$v'(x) = \sqrt{2\lambda[F(\rho) - F(v(x))]}, \quad x \in (0, \frac{1}{2}), \quad (11)$$

and since $F \in C^1(q, \rho)$ and $v \in C^1(0, \frac{1}{2})$, we observe that $v' \in C^1(0, \frac{1}{2})$. Differentiating again, we find that

$$-v''(x) = \lambda f(v(x)), \quad x \in (0, \frac{1}{2}).$$

Hence, since f is continuous, $v(\frac{1}{2}) = \rho$ and $v'(\frac{1}{2}) = 0$, we conclude that $v \in C^2(0, 1) \cap C^1[0, 1]$ by our extension of v . Moreover, from (11), we observe that $v'(0) = \sqrt{2\lambda[F(\rho) - F(q)]}$ and from (5), this implies

$$v'(0) = \sqrt{\lambda}\gamma \frac{v(0)}{(v(0) - A)^2 + \epsilon}.$$

Our extension of v guarantees that

$$v'(1) = -\sqrt{\lambda}\gamma \frac{v(1)}{(v(1) - A)^2 + \epsilon}.$$

Hence, v is a positive solution to (4) with $v(0) = q = v(1)$ and $v(\frac{1}{2}) = \rho$ as desired.

3. Numerical results

Using Mathematica, we may numerically solve for (λ, ρ) pairs which simultaneously satisfy (5) and (6). To do so, we implement the following algorithm:

- (1) Choose $\rho \in (0, 1)$.
- (2) For a given ρ , use nonlinear solver to solve (6) for q .
- (3) For a given ρ and its corresponding value for q , use (5) to find λ .
- (4) Plot (λ, ρ) pair.

We select 500 equally spaced values for ρ in $(0, 1)$. For a fixed ρ , we use the FindRoot command in Mathematica, which employs Newton's method, to solve (6) for q with an accuracy of 10^{-4} . Some examples of bifurcation curves with a fixed value of $\epsilon = .1$, and different values for γ and A are provided in Figures 4–7. Parameter values are chosen to illustrate the variety of possible bifurcation curves, but are not otherwise known to be of ecological significance.

We remind the reader, as in Remark 3, that the bifurcation curves provided in Figures 4–7 are the bifurcation curves for positive, symmetric solutions only. Any reference in this section to a solution should be interpreted as a reference to a positive, symmetric solution.

We first illustrate in Figure 4 how the number of solutions to (4) may depend on A . For $\epsilon = .1$ and $\gamma = .1$, we plot in Figure 4 the bifurcation curve for two differing values of A . When $A = .5$, we observe that for sufficiently small λ , there are no solutions, while for λ sufficiently large, there is a unique solution. We notice, however, that when A is decreased to $A = .25$, we now have multiple positive, symmetric solutions for a range of λ .

Secondly, we illustrate in Figures 5 and 6 how multiplicity of solutions may occur. In Figure 5, we first observe how the structure of these ranges of λ for which multiple solutions exist can also vary depending on A . Specifically, in Figure 5, left, for sufficiently small λ there are no solutions, then for the proceeding ranges of λ there is one solution, three solutions, and one solution. Similarly, in Figure 5,

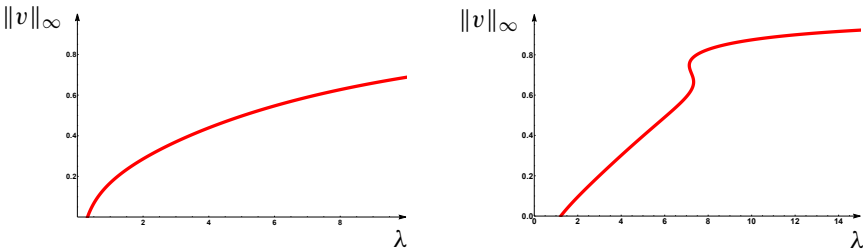


Figure 4. For $\gamma = .1$, we observe that varying values of A introduce multiplicity of solutions: $A = .5$ (left) and $A = .25$ (right).

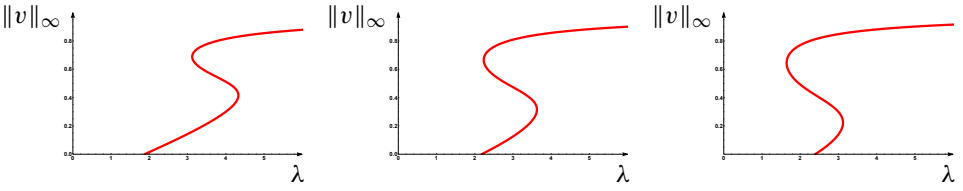


Figure 5. For $\gamma = .1$, we observe that the multiplicity of solutions and the range of λ for which certain multiplicities exist change as A is varied: $A = .15$ (left), $A = .1$ (middle), $A = .05$ (right).

middle, for sufficiently small λ there are no solutions, then for the proceeding values of λ there are three solutions then one solution. In **Figure 5**, right, for sufficiently small λ there are no solutions, then for the proceeding ranges of λ there are two solutions, three solutions, and one solution.

Building from **Figure 5**, we illustrate in **Figure 6** the multiplicity of solutions that can occur for certain parameter regimes. When $\gamma = \epsilon = A = .1$, we numerically solve (5), (6) for ρ, q when $\lambda = 3$. We find solutions

$$\begin{aligned}
 (\rho_1, q_1) &= (0.12558361681607486, 0.08633543422628163), \\
 (\rho_2, q_2) &= (0.4731562619350849, 0.38016022177071546), \\
 (\rho_3, q_3) &= (0.8091464421614853, 0.7490510239916139).
 \end{aligned}$$

In **Figure 6**, we illustrate the correspondence between the multiple points $(3, \rho_i)$, $i = 1, 2, 3$, on the bifurcation curve and the multiple solutions v_i , $i = 1, 2, 3$, of (4), with $v_i(0) = q_i = v_i(1)$ and $\|v_i\|_\infty = v_i(\frac{1}{2}) = \rho_i$.

Finally, we illustrate in **Figure 7** how large values of γ may force uniqueness of solutions. For $\epsilon = .1$ and $\gamma = 10$, we observe that even a large change in the value of A does not change the shape of the graph. Thus, we conjecture that if $\gamma \gg 1$, there exists $\lambda^* > 0$, so that (4) has no solution for $0 < \lambda < \lambda^*$, has a unique solution for every $\lambda > \lambda^*$, and $\rho(\lambda)$ is strictly increasing.

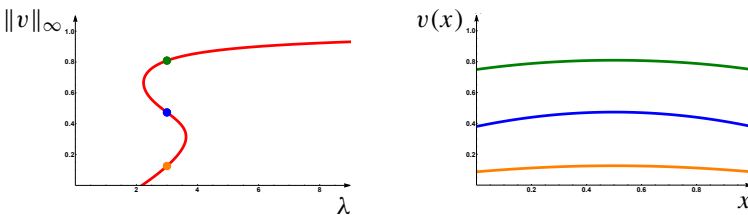


Figure 6. For $\gamma = \epsilon = A = .1$, we observe there are multiple solutions when $\lambda = 3$. Left: bifurcation curve highlighting points $(3, \rho_i)$, $i = 1, 2, 3$. Right: solutions v_i of (4) with $\lambda = 3$.

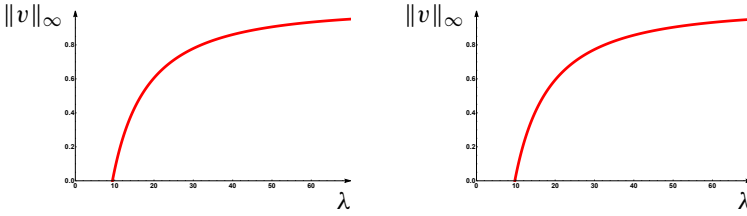


Figure 7. For $\gamma = 10$, we observe that even large perturbations of the parameter A do not introduce multiplicity of solutions: $A = .5$ (left), $A = .000005$ (right).

4. Biological interpretation

Given the numerical results in [Section 3](#), we consider now the biological implications. Recall that $\lambda = r\ell^2/D$ and $\gamma = S^*/\sqrt{rD}$, which shows that λ is proportional to the square of the patch size ℓ and γ is proportional to the hostility of the matrix S^* .

First, we observe that, in all numerical cases explored, regardless of our choices of γ or A , there exist $\lambda^* > 0$ such that (4) has no solution for $\lambda < \lambda^*$. In biological terms, there exists some minimum patch size $\ell^* = \sqrt{D\lambda^*/r}$ that will support a population. Furthermore, in all cases, we observe that for λ sufficiently large, there exists a unique steady state. This illustrates a decreasing role of boundary effects on a population as the habitat grows larger. We note that such behavior is consistent with theoretical results proved in [\[Fonseka et al. 2019\]](#) in the case of UDDD.

Secondly, we observe that when γ is sufficiently small, the parameter A has a large influence on the shape of the bifurcation curve, in particular, by introducing multiple steady states. This phenomena is biologically interesting, as this implies that the population density that induces maximum dispersal on the boundary also determines whether multiple steady states of the population exist, and if so, for what ranges of patch sizes the steady states persist. On the other hand, when γ is sufficiently large, we observe that changes in the parameter A do not influence the shape of the bifurcation curve, and in particular, do not introduce multiple steady states. This suggests that as the outside matrix becomes increasingly hostile, any individual leaving the population dies almost immediately, and thus, the habitat behaves almost identically to one with a lethal boundary.

Acknowledgements

This project was initiated when the authors were at the University of North Carolina at Greensboro under the direction of Professor R. Shivaji and was supported by the NSF grant (DMS-1516560). We thank Shivaji for his guidance throughout this project.

References

- [Cantrell and Cosner 2003] R. S. Cantrell and C. Cosner, *Spatial ecology via reaction-diffusion equations*, John Wiley & Sons, Chichester, 2003. [MR](#) [Zbl](#)
- [Cantrell et al. 1998] R. S. Cantrell, C. Cosner, and W. F. Fagan, “Competitive reversals inside ecological reserves: the role of external habitat degradation”, *J. Math. Biol.* **37**:6 (1998), 491–533. [MR](#) [Zbl](#)
- [Cronin et al. 2019] J. T. Cronin, J. Goddard, and R. Shivaji, “Effects of patch–matrix composition and individual movement response on population persistence at the patch level”, *Bull. Math. Biol.* **81**:10 (2019), 3933–3975. [MR](#)
- [Enfjäll and Leimar 2005] K. Enfjäll and O. Leimar, “Density-dependent dispersal in the Glanville fritillary, *Melitaea cinxia*”, *Oikos* **108**:3 (2005), 465–473.
- [Fisher 1937] R. A. Fisher, “The wave of advance of advantageous genes”, *Ann. Eugenics* **7**:4 (1937), 355–369. [JFM](#)
- [Fonseka et al. 2019] N. Fonseka, J. Goddard, II, Q. Morris, and R. Shivaji, “On the effects of the exterior matrix hostility and a u-shaped density dependent dispersal on a diffusive logistic growth model”, preprint, 2019. To appear in *Discrete Cont. Dyn. Syst. Ser. S*.
- [Goddard et al. 2018] J. Goddard, II, Q. Morris, R. Shivaji, and B. Son, “Bifurcation curves for singular and nonsingular problems with nonlinear boundary conditions”, *Electron. J. Differential Equations* (2018), art. id. 26. [MR](#) [Zbl](#)
- [Goddard et al. \geq 2020] J. Goddard, II, J. Price, and R. Shivaji, “Analysis of steady states for classes of reaction-diffusion equations with u-shaped density dependent dispersal on the boundary”, in preparation.
- [Kareiva 1983] P. M. Kareiva, “Local movement in herbivorous insects: applying a passive diffusion model to mark-recapture field experiments”, *Oecologia* **57**:3 (1983), 322–327.
- [Kim et al. 2009] S.-Y. Kim, R. Torres, and H. Drummond, “Simultaneous positive and negative density-dependent dispersal in a colonial bird species”, *Ecology* **90**:1 (2009), 230–239.
- [Kolmogorov et al. 1937] A. Kolmogorov, I. Petrovskii, and N. Piskunov, “Study of a diffusion equation that is related to the growth of a quality of matter and its application to a biological problem”, *Byul. Mosk. Gos. Univ. Ser. A Mat. Mekh.* **1**:6 (1937), 1–26. In Russian. [Zbl](#)
- [Kuussaari et al. 1998] M. Kuussaari, I. Saccheri, M. Camara, and I. Hanski, “Allee effect and population dynamics in the glanville fritillary butterfly”, *Oikos* **82**:2 (1998), 384–392.
- [Laetsch 1971] T. Laetsch, “The number of solutions of a nonlinear two point boundary value problem”, *Indiana Univ. Math. J.* **20** (1971), 1–13. [MR](#) [Zbl](#)
- [Skellam 1951] J. G. Skellam, “Random dispersal in theoretical populations”, *Biometrika* **38** (1951), 196–218. [MR](#) [Zbl](#)
- [Turchin and Thoeny 1993] P. Turchin and W. Thoeny, “Quantifying dispersal of southern pine beetles with mark-recapture experiments and a diffusion model”, *Ecol. Appl.* **3**:1 (1993), 187–198.

Received: 2018-05-14

Revised: 2019-06-13

Accepted: 2019-10-02

morrisqa@appstate.edu

Swarthmore College Swarthmore, PA, United States

Current address:

Appalachian State University, Boone, NC, United States

jjnash@uw.edu

The University of North Carolina at Greensboro,
Greensboro, NC, United States

payneca@wssu.edu

Department of Mathematics, Winston-Salem State University,
Winston-Salem, NC, United States

INVOLVE YOUR STUDENTS IN RESEARCH

Involve showcases and encourages high-quality mathematical research involving students from all academic levels. The editorial board consists of mathematical scientists committed to nurturing student participation in research. Bridging the gap between the extremes of purely undergraduate research journals and mainstream research journals, *Involve* provides a venue to mathematicians wishing to encourage the creative involvement of students.

MANAGING EDITOR

Kenneth S. Berenhaut Wake Forest University, USA

BOARD OF EDITORS

Colin Adams	Williams College, USA	Robert B. Lund	Clemson University, USA
Arthur T. Benjamin	Harvey Mudd College, USA	Gaven J. Martin	Massey University, New Zealand
Martin Bohner	Missouri U of Science and Technology, USA	Mary Meyer	Colorado State University, USA
Amarjit S. Budhiraja	U of N Carolina, Chapel Hill, USA	Frank Morgan	Williams College, USA
Pietro Cerone	La Trobe University, Australia	Mohammad Sal Moslehian	Ferdowsi University of Mashhad, Iran
Scott Chapman	Sam Houston State University, USA	Zuhair Nashed	University of Central Florida, USA
Joshua N. Cooper	University of South Carolina, USA	Ken Ono	Univ. of Virginia, Charlottesville
Jem N. Corcoran	University of Colorado, USA	Yuval Peres	Microsoft Research, USA
Toka Diagana	University of Alabama in Huntsville, USA	Y.-F. S. Pétermann	Université de Genève, Switzerland
Michael Dorff	Brigham Young University, USA	Jonathon Peterson	Purdue University, USA
Sever S. Dragomir	Victoria University, Australia	Robert J. Plemmons	Wake Forest University, USA
Joel Foisy	SUNY Potsdam, USA	Carl B. Pomerance	Dartmouth College, USA
Erin W. Fulp	Wake Forest University, USA	Vadim Ponomarenko	San Diego State University, USA
Joseph Gallian	University of Minnesota Duluth, USA	Bjorn Poonen	UC Berkeley, USA
Stephan R. Garcia	Pomona College, USA	József H. Przytycki	George Washington University, USA
Anant Godbole	East Tennessee State University, USA	Richard Rebarber	University of Nebraska, USA
Ron Gould	Emory University, USA	Robert W. Robinson	University of Georgia, USA
Sat Gupta	U of North Carolina, Greensboro, USA	Javier Rojo	Oregon State University, USA
Jim Haglund	University of Pennsylvania, USA	Filip Saidak	U of North Carolina, Greensboro, USA
Johnny Henderson	Baylor University, USA	Hari Mohan Srivastava	University of Victoria, Canada
Glenn H. Hurlbert	Virginia Commonwealth University, USA	Andrew J. Sterge	Honorary Editor
Charles R. Johnson	College of William and Mary, USA	Ann Trenk	Wellesley College, USA
K. B. Kulasekera	Clemson University, USA	Ravi Vakil	Stanford University, USA
Gerry Ladas	University of Rhode Island, USA	Antonia Vecchio	Consiglio Nazionale delle Ricerche, Italy
David Larson	Texas A&M University, USA	John C. Wierman	Johns Hopkins University, USA
Suzanne Lenhart	University of Tennessee, USA	Michael E. Zieve	University of Michigan, USA
Chi-Kwong Li	College of William and Mary, USA		

PRODUCTION

Silvio Levy, Scientific Editor

Cover: Alex Scorpan

See inside back cover or msp.org/involve for submission instructions. The subscription price for 2020 is US \$205/year for the electronic version, and \$275/year (+\$35, if shipping outside the US) for print and electronic. Subscriptions, requests for back issues and changes of subscriber address should be sent to MSP.

Involve (ISSN 1944-4184 electronic, 1944-4176 printed) at Mathematical Sciences Publishers, 798 Evans Hall #3840, c/o University of California, Berkeley, CA 94720-3840, is published continuously online. Periodical rate postage paid at Berkeley, CA 94704, and additional mailing offices.

Involve peer review and production are managed by EditFlow[®] from Mathematical Sciences Publishers.

PUBLISHED BY

 **mathematical sciences publishers**

nonprofit scientific publishing

<http://msp.org/>

© 2020 Mathematical Sciences Publishers

involve

2020

vol. 13

no. 1

Structured sequences and matrix ranks	1
CHARLES JOHNSON, YAOXIAN QU, DUO WANG AND JOHN WILKES	
Analysis of steady states for classes of reaction-diffusion equations with hump-shaped density-dependent dispersal on the boundary	9
QUINN MORRIS, JESSICA NASH AND CATHERINE PAYNE	
The L-move and Markov theorems for trivalent braids	21
CARMEN CAPRAU, GABRIEL COLOMA AND MARGUERITE DAVIS	
Low stages of the Taylor tower for r-immersions	51
BRIDGET SCHREINER, FRANJO ŠARČEVIĆ AND ISMAR VOLIĆ	
A new go-to sampler for Bayesian probit regression	77
SCOTT SIMMONS, ELIZABETH J. MCGUFFEY AND DOUGLAS VANDERWERKEN	
Characterizing optimal point sets determining one distinct triangle	91
HAZEL N. BRENNER, JAMES S. DEPRET-GUILLAUME, EYVINDUR A. PALSSON AND ROBERT W. STUCKEY	
Solutions of periodic boundary value problems	99
R. AADITH, PARAS GUPTA AND JAGAN MOHAN JONNALAGADDA	
A few more trees the chromatic symmetric function can distinguish	109
JAKE HURYN AND SERGEI CHMUTOV	
One-point hyperbolic-type metrics	117
MARINA BOROVIKOVA, ZAIR IBRAGIMOV, MIGUEL JIMENEZ BRAVO AND ALEXANDRO LUNA	
Some generalizations of the ASR search algorithm for quasitwisted codes	137
NUH AYDIN, THOMAS H. GUIDOTTI, PEIHAN LIU, ARMIYA S. SHAIKH AND ROBERT O. VANDENBERG	
Continuous factorization of the identity matrix	149
YUYING DAI, ANKUSH HORE, SIQI JIAO, TIANXU LAN AND PAVLOS MOTAKIS	
Almost excellent unique factorization domains	165
SARAH M. FLEMING AND SUSAN LOEPP	